Eye Position Compensation Improves Estimates of Response Magnitude and Receptive Field Geometry in Alert Monkeys

Yamei Tang, Alan Saul, Moshe Gur, Stephanie Goei, Elsie Wong, Bilgin Ersoy and D. Max Snodderly

J Neurophysiol 97:3439-3448, 2007. First published Mar 7, 2007; doi:10.1152/jn.00881.2006

J Neurophysiol 97: 3439–3448, 2007.
First published March 7, 2007; doi:10.1152/jn.00881.2006.

Eye Position Compensation Improves Estimates of Response Magnitude and Receptive Field Geometry in Alert Monkeys

Yamei Tang,[1,2] Alan Saul,[1] Moshe Gur,[3] Stephanie Goei,[1] Elsie Wong,[1] Bilgin Ersoy,[4] and D. Max Snodderly[1,5]
[1]*Department of Ophthalmology, Medical College of Georgia, Augusta, Georgia;* [2]*Department of Neurology, The Second Affiliated Hospital, Sun Yat-Sen University, Guangzhou, China;* [3]*Department of Biomedical Engineering, Technion, Haifa, Israel;* [4]*Department of Cognitive and Neural Systems, Boston University, Boston, Massachusetts; and* [5]*Department of Human Ecology and Institute for Neuroscience, University of Texas, Austin, Texas*

Submitted 18 August 2006; accepted in final form 24 February 2007

Tang Y, Saul A, Gur M, Goei S, Wong E, Ersoy B, Snodderly DM. Eye position compensation improves estimates of response magnitude and receptive field geometry in alert monkeys. *J Neurophysiol* 97: 3439–3448, 2007. First published March 7, 2007; doi:10.1152/jn.00881.2006. Studies of visual function in behaving subjects require that stimuli be positioned reliably on the retina in the presence of eye movements. Fixational eye movements scatter stimuli about the retina, inflating estimates of receptive field dimensions, reducing estimates of peak responses, and blurring maps of receptive field subregions. Scleral search coils are frequently used to measure eye position, but their utility for correcting the effects of fixational eye movements on receptive field maps has been questioned. Using eye coils sutured to the sclera and preamplifiers configured to minimize cable artifacts, we reexamined this issue in two rhesus monkeys. During repeated fixation trials, the eye position signal was used to adjust the stimulus position, compensating for eye movements and correcting the stimulus position to place it at the desired location on the retina. Estimates of response magnitudes and receptive field characteristics in V1 and in LGN were obtained in both compensated and uncompensated conditions. Receptive fields were narrower, with steeper borders, and response amplitudes were higher when eye movement compensation was used. In sum, compensating for eye movements facilitated more precise definition of the receptive field. We also monitored horizontal vergence over long sequences of fixation trials and found the variability to be low, as expected for this precise behavior. Our results imply that eye coil signals can be highly accurate and useful for optimizing visual physiology when rigorous precautions are observed.

INTRODUCTION

Control of stimulus position on the retina represents a challenge for investigations of visual processing in behaving monkeys. Previous studies showed that receptive fields of neurons in primary visual cortex (V1) are fixed on the retina and move in space with movements of the eye (Gur and Snodderly 1987, 1997). Changes in eye position interfere with estimation of receptive field substructure and cause inflated estimates of receptive field dimensions and underestimates of peak response rates. These errors in turn lead to misconceptions about the coding properties of the neurons. Furthermore, lack of control of stimulus position on the retina can make it extremely difficult to stimulate the cells with the smallest receptive fields and the most specific stimulus requirements, leading to biased samples of neuronal populations (Gur and Snodderly, unpublished observations). Achieving precise stimulus control is crucial for studying receptive fields in the fovea, which have received little attention because of their small sizes.

Scleral search coils are commonly used to provide measurements of eye position of behaving monkeys (Robinson 1963). Stimulus position can be adjusted using the eye position signal to compensate for eye movements and to place the stimulus at the desired location on the retina (Gur and Snodderly 1987). Based on coils that were not sutured to the sclera, Read and Cumming (2003) reported that eye coil signals were not veridical and that compensating for eye movements did not reduce measured receptive field sizes. A study of V1 receptive fields in behaving monkeys using sutured search coils, but correcting eye position off-line, also concluded that correcting for measured eye position does not improve receptive field maps across the population (Tsao et al. 2003). Because of its methodological importance, we reexamined this question, using eye coils sutured to the globe and an eye position monitoring system configured for maximum accuracy. We found that correction of stimulus position using scleral search coils significantly improved measurement of response magnitudes and receptive field characteristics for both the lateral geniculate nucleus (LGN) and for cortical area V1.

METHODS

Two adult female monkeys (*Macaca mulatta*) were trained to fixate on a light-emitting diode (LED) for a water reward. Once they had learned the basic task, a head-holding implant and a recording well were surgically attached to the skull under deep anesthesia and sterile conditions. All procedures adhered to National Institutes of Health guidelines and were approved by the Animal Care and Use Committee of the Medical College of Georgia.

Eye coil implants

Scleral search coils with three turns (left eye of M46) or four turns (right eye of M46 and both eyes of M49) were implanted in the monkeys' eyes using the basic approach developed by Judge et al. (1980). During the experiments we changed from coils with three turns to those with four turns to increase the signal. We also fabricated the coils with larger-diameter wire (0.36-mm OD, 0.19-mm ID; code

Address for reprint requests and other correspondence: A. Saul, Department of Ophthalmology, Medical College of Georgia, Augusta, GA 30912 (E-mail: asaul@mcg.edu).

The costs of publication of this article were defrayed in part by the payment of page charges. The article must therefore be hereby marked "*advertisement*" in accordance with 18 U.S.C. Section 1734 solely to indicate this fact.

AS634, Cooner Wire, Chatsworth, CA), which decreased the resistance and noise and was more durable.

The eye coils were sutured to the sclera with four 8–0 nylon sutures in the quadrants between the rectus muscle insertions, using a spatula needle. To maximize the holding strength of the sutures, we inserted the needle into the sclera parallel to the coil on each side and the sutures were tied over the coil (Fig. 1). By rotating the eye, as well as by pulling on the leads, secure placement and lack of slippage was confirmed. A hairpin loop was created in a lateral conjunctival pouch by pushing the wire lead back into the orbit with a muscle hook. This loop provided strain relief, allowing the eye to move freely without binding from the leads. The side of the loop adjacent to the globe was also sutured to the globe just posterior to the coil and just superior to the lateral rectus (location indicated by the thick arrow of Fig. 1). This suture ensured that flexion of the leads during eye rotation occurred in an uninterrupted stretch of wire, rather than at the junction between the leads and the coil, which is a mechanical weak point. The leads were threaded into a postmortem needle and pulled out of the orbit through the anterolateral cartilaginous wall and through a small incision in the skin behind the orbit, just above the zygomatic arch. Another suture was placed here to secure the leads to the temporal musculature. Again using the postmortem needle, the leads were pulled to the top of the head underneath the temporal muscle, as close to the skull as possible. Finally, the leads were secured to connectors embedded in the acrylic head-holding implant. The overall strategy was to implant the leads in a way that would minimize movement by muscular contractions and skin movements because movement of the leads in the magnetic field generates artifactual signals in the eye position output.

Characteristics of the eye position monitor

To characterize system performance, a four-turn eye coil, with the same size and with impedance similar to one of the eye coils that was implanted on a monkey's eye, was rigidly suspended in the magnetic field (we refer to this as a *dummy coil*). The eye coil monitor (Remmel Labs EM7) was set to the same gain used with the monkeys and the same high-frequency cutoff of 320 Hz. Noise with the dummy coil was <0.5 minarc peak-to-peak when sampled at our standard rate of 200 Hz. A useful feature of the Remmel Labs system is a $\times 40$ preamplifier positioned close to each eye of the monkey; the preamplifiers are connected to thick coaxial cables (RG58/U) to carry the signal to the conditioning electronics and additional gain stages. The thick cables reduce artifacts caused by cable movements in the magnetic field and the preamplification also minimizes these artifacts as well as the contributions of noise pickup by the cables, with the result that the combination improves the signal-to-noise ratio.

To evaluate the long-term stability of the system, signals from a four-turn dummy coil were recorded for repeated 5-s trials over a period of about 30 min. We found that position was stable across the whole run for the dummy coil, with an intertrial SD of the trial means of 0.05 minarc ($n = 87$) and mean intratrial SD of 0.1 minarc. These results were replicated on three separate days.

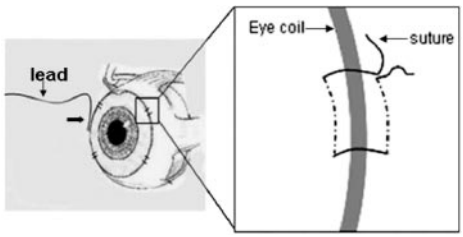

FIG. 1. Eye coil sutured to the sclera. This is a view of the right eye seen from the medial side. Enlargement illustrates how the coil was sutured. Dashed lines indicate the path taken by the suture within the sclera. Coils were placed as far posterior as possible, just anterior to the muscle insertions. Lead from the coil was pushed back into the orbit in a hairpin loop and the side of the loop adjacent to the globe (shown with thick arrow) was fastened to the globe with an additional suture. (Figure modified from a drawing by Skalar Medical, used with permission.)

Experimental procedures

At the beginning of each recording session, the eye position monitor was calibrated by having the monkey look at targets placed 5° apart. During experimental sessions, the fixation target was a small red LED placed directly in front of the animal at a distance of 114 or 172 cm. The monkeys had to maintain fixation for 5 s within a ± 60 minarc window. A deviation in eye position $>1°$ that lasted for >100 ms resulted in cancellation of the trial. Briefer excursions out of the window arising from blinks and other looping saccades (e.g., Snodderly 1987; Fig. 2), which quickly returned the eye to the initial position, did not cancel trials, so that monkeys were not punished and we were able to retain valuable data.

Single units were recorded extracellularly with fine platinum–tungsten fibers insulated with quartz (Reitboeck 1983; Thomas Recording, Giessen, Germany) having impedances of 1–5 MΩ at 1 kHz. Recorded signals were amplified and band-pass filtered (300–5,000 Hz) by TDT hardware (Tucker-Davis Technologies, Alachua, FL) using Brainware software on a personal computer. Only well-isolated single units in V1 and LGN were used for mapping. In V1, the sample was biased toward cells with no ongoing activity because it simplified measurement of receptive field dimensions.

A separate computer with a VSG card (Cambridge Research Systems, Kent, UK) was used for stimulus generation. Stimuli were presented on a 21-in. Sony monitor with a 160-Hz refresh rate (noninterlaced), at a distance of 114 or 172 cm from the monkey. The eye position signal, sampled at 200 Hz, was added to the stimulus position signal from the computer at the beginning of each video frame to compensate for changes in eye position during the trial (Gur and Snodderly 1987, 1997; Snodderly and Gur 1995). The overall time lag from sampling eye position to correcting the stimulus position was typically 5–6 ms and, in the worst case, 10 ms. Because of this delay, position compensation lags slightly behind the movement of the eye during saccades (Gur and Snodderly 1987). Eye position compensation could be turned on and off under program control.

Measurement of response magnitude and receptive field characteristics

Bright and dark bars having optimal orientation, color, and spatial configuration were swept forward and back across the receptive field at speeds ranging from 1 to 10°/s (mean speed was 3°/s). Bar widths were between 4 and 40 minarc, most often 15 minarc. Trials with compensation alternated with trials without compensation in runs lasting 5–20 min for the LGN data. V1 data were collected in pairs of runs consisting of separate blocks of trials with and without compensation. Each cell could potentially provide data from two directions and two contrasts. The direction/contrast pair with the maximum amplitude averaged over the trials with and without compensation was used for all comparisons. Histograms showing where spikes occurred during the stimulus sweeps were compiled from 25 to 200 repetitions of the stimulus (Fig. 2, *C* and *D*). Binwidths were about 10 ms. Data were rejected if the mean of the peak response over all sweeps did not differ from 0 at the 95% level (*t*-test).

The goal was to test whether receptive fields were smeared by eye movements in the absence of compensation (Fig. 2, *B* and *D*). Receptive field width, response amplitude, and slopes of the histograms at the receptive field borders were measured for this purpose.

Several methods to estimate the width of receptive fields from response histograms were tested. These methods included taking the width at a criterion level relative to the peak, using the zeros of the

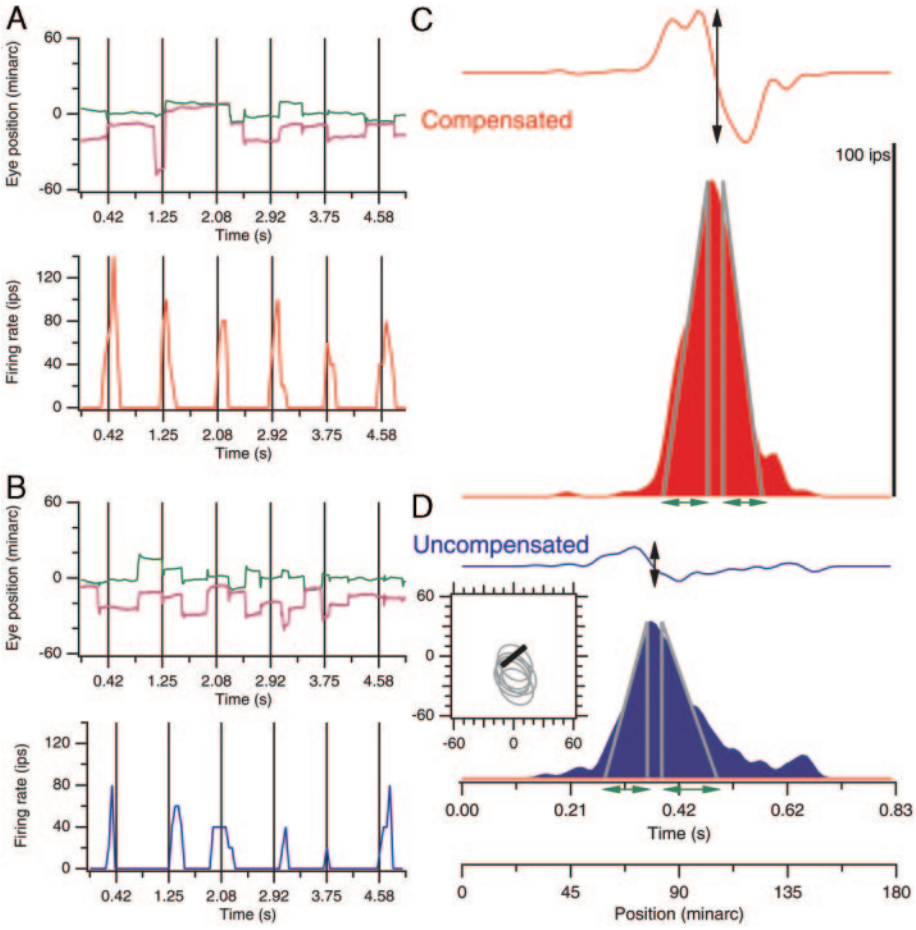

FIG. 2. Measuring effects of eye movements on receptive field parameters. A primary visual cortex (V1) complex cell from M49 was tested with a 30 × 4 minarc bar sweeping back and forth across its receptive field with and without eye position compensation. *A*: horizontal (green) and vertical (magenta) components of the eye position signal are shown for a trial with compensation for eye movements, with responses below. Vertical lines mark the centers of the stimulus sweeps. *B*: eye position and responses are shown in the same format for a trial without eye movement compensation. *C*: solid red histogram shows the average response over all upward stimulus sweeps for data collected with compensation for eye position. Above the histogram is the smoothed derivative of the histogram. Peak and trough of the derivative are the maximum slopes of the rise and fall of the histogram and the length of the black arrow from the peak to the trough indicates the sum of the absolute values of these slopes. Gray lines over the histogram and the green arrows illustrate the border width measure derived from these slopes. *D*: average responses in the uncompensated condition are shown in blue. *Inset*: receptive field (gray ovals) in relative visual field coordinates (scales are in minarcs) for the trial shown in *B* at each of the 6 locations where the bar crossed the center of its sweep, with the stimulus bar drawn in black. Major position scatter is on the vertical axis.

second derivative to mark borders, fitting the cumulative histogram with sigmoidal functions, or equivalently fitting functions directly to the histogram. No single method was clearly superior to all others, so we present results from two methods here. The first method was similar to that used by Read and Cumming (2003), fitting Gaussians to the response histogram. We used Gaussians with four parameters: background activity level, amplitude, center, and width. To ensure an adequate fit, results were rejected if the correlation coefficient between the fit and the data was <0.9. The receptive field width was taken as the full width at 5% of the peak (other criterion values produce similar results with different scaling). In the second method, receptive field width was defined as the full width of smoothed histograms at a height of 1 SD of the amplitude values. Note that this measure is not equivalent to the SD of the Gaussian density function approximating the response histogram and it does not assume a specific spatial shape of the response histogram.

Estimates of response strength and position sensitivity were obtained from the spike histograms. To measure response strength, the averaged raw histogram was smoothed by a Gaussian with a half-width of 14 ms and the peak firing rate was taken as an estimate of response amplitude. For the sensitivity, we computed how quickly amplitude changed with position. Maximum slopes of the rising and falling sides of the histogram were measured. The raw histogram was differentiated, smoothed with a Gaussian with a half-width of 14 ms, and the peak positive and negative values were used (Fig. 2, *C* and *D*; double-headed black arrows). We computed raw slopes (with units of ips/minarc), that depend on both amplitude and width of the histograms, as well as normalized slopes (with units of 1/minarc), after setting the height of the histograms to 1. The raw absolute slopes are a measure of the maximum sensitivity of the neuron to small displacements of the retinal image. The sum of the reciprocals of the normalized absolute slopes provides a measure closely related to width, but one that is more sensitive than total receptive field width to the effects of small eye movements. We refer to this as *border width* because it is an estimate of the total width of the regions within which the response rises and falls rapidly. The border width measure is illustrated in Fig. 2 by the gray lines and green arrows. The angled lines indicate the maximum slopes and they pass through the points on the histogram where these maximum slopes are achieved. The vertical lines indicate the points where the angled lines cross the peak value of the histogram and they designate the central edges of the borders. The distance between the intersections of the angled and the vertical gray lines with the horizontal axis is the border width (green arrows, Fig. 2, *C* and *D*). Values reported herein are the sums of the border widths of the rising and falling sides of the histogram.

Off-line corrections

For comparison with the results from on-line eye position compensation, histograms from uncompensated trials were corrected off-line. The position of the bar on the retina was calculated and the appropriate bin along the sweep was updated by adding spikes and accounting for the time spent in that bin. Bin counts were then normalized by these durations. Because of response latency, it is the stimulus position on the retina at times before spikes that counts. We did not have an estimate for latency for each individual cell, so we used a representative latency of 50 ms for all cells for the purposes of these calculations. Details of the algorithm involved taking, for each trial, the eye position component along the axis of the bar movement and subtracting the eye position from the nominal stimulus. This retinal location corresponds to a particular bin in the spike histogram 50 ms later. An additional histogram kept track of how long the stimulus was

in each bin. After accumulating all the trials, the spike histogram was divided by the time histogram to compute spikes/unit time at each retinal location.

Programs for analysis were written in Igor Pro (WaveMetrics, Lake Oswego, OR). Comparisons between conditions were paired *t*-tests except where noted.

RESULTS

Effects of compensation for fixational eye movements

Eye movements that are always present, even while fixating, cause visual stimuli to fall at scattered points on the retina (Fig. 2, *inset*). Compensating for fixational eye movements using the eye position signal reduces this scatter. Figure 2, *A* and *B* shows responses during trials with and without compensation. With compensation (red), responses occurred regularly and reliably, despite numerous small eye movements. In the trial illustrated in Fig. 2*A*, eye position varied over about 20 minarc, but, because the stimulus was shifted on the screen to compensate for eye position, the response occurred at the expected time, peaking just after the stimulus crossed the middle of its sweep. In contrast, without compensation (Fig. 2*B*), responses were not as reliable and did not always occur at the expected times. Because the fixation position was a bit low, the receptive field was shifted down on the stimulus monitor (*inset*) and responses were generated later in the downward sweeps and earlier in the upward sweeps. Across many trials, eye movement patterns did not differ between compensated and uncompensated trials because the stimulus was irrelevant for the monkeys' behaviors.

We measured the improvement that compensation provides by comparing receptive field widths, amplitudes, and slopes between histograms computed from trials with and without compensation (Fig. 2, *C* and *D*). One striking difference between compensated and uncompensated histograms was in rise and fall times: the sharp borders of receptive fields were smeared out by the eye movements. We measured the slopes of the histograms from their derivatives. The raw slope combines the width and amplitude measures, both of which were affected by eye movements, into a single index. We also normalized the slope, dividing by the amplitude, which yields values with units of minarc^{-1}. The reciprocal of this normalized slope is the distance over which the histogram rises and falls, referred to here as *border width*. It is related to the width of the receptive field, but ignores any middle portion where the response does not change rapidly.

Eye movement amplitudes

Horizontal and vertical position were stored for the dominant eye, except in the measurements of vergence for which horizontal position in each eye was recorded. The typical behavior during a 5-s trial was that the fixation point was acquired during the initial 500 ms, followed by variably stable fixation until the final second or so, when monkeys tend to concentrate to detect the offset of the LED. When combining dozens of trials, eye position deviated from its base level relatively rarely, but did so with magnitudes of 30–60 minarc on many of those rare occasions. This creates nonnormal distributions of eye position (Fig. 3). In particular, the distributions were kurtotic, highly peaked around the mode with strong tails (see legend). They also tended to be skewed because monkeys tended to make eye movements asymmetrically. The vertical component of eye position usually showed larger deviations than the horizontal component as described previously (Barash et al. 1998; Snodderly 1987). No eye movement differences were observed between compensated and uncompensated conditions.

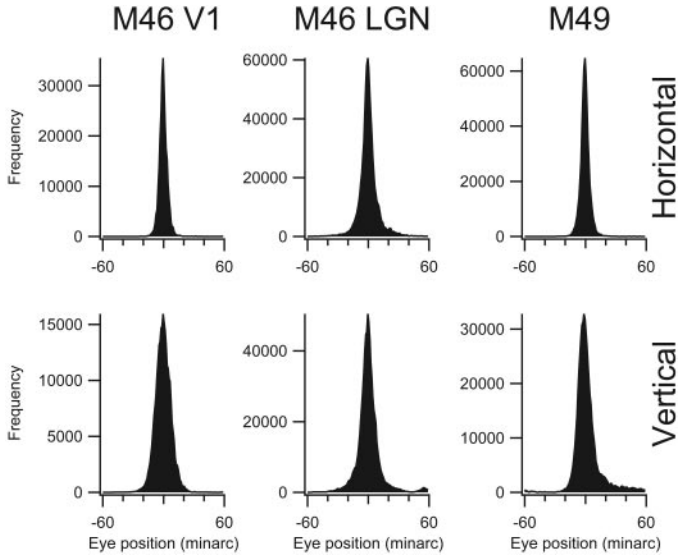

FIG. 3. Eye position distributions. Horizontal (*top*) and vertical (*bottom*) components of eye position were combined across all data presented in this study, separating the V1 and lateral geniculate nucleus (LGN) experiments from M46. Eye positions shown here are relative to the modal eye position for each run because arbitrary offsets differed between runs. SD (in minarc), kurtosis (in excess of 3), and interquartile ranges (in minarc) for these distributions were: M46 V1 horizontal (4.7, 25, 4.6); M46 V1 vertical (8.0, 3.8, 9.7); M46 LGN horizontal (10.1, 6.7, 7.9); M46 LGN vertical (12.3, 6.6, 9.5); M49 horizontal (5.4, 21.5, 4.2); M49 vertical (12.8, 5.9, 10.3).

The two monkeys tested for this report differed in their behaviors and one monkey tested in separate series of experiments a year apart varied in her behavior between those experiments. We computed the absolute deviation of eye position because the SD (see figure legend) tends to overemphasize the outliers. Combining horizontal and vertical eye movements showed that monkey M46 had an average absolute deviation of 6.5 minarc during the period when we recorded from her cortex, but increased to 9.5 minarc during the LGN testing a year later. Monkey M49 had an average deviation of 12.0 minarc. She had a much higher frequency of saccades, close to 3 Hz, as opposed to M46 who rarely made saccades ($<$1 Hz), especially during the V1 testing.

Receptive field geometry and response magnitudes

Widths of receptive field centers were measured in compensated and uncompensated conditions from a population of 32 cortical cells from monkeys M46 (13 cells) and M49 (19 cells) and 30 LGN cells from M46. Of the V1 cells, four were simple, 23 were complex, and five were unclassified. Simple cells had nonoverlapping bright-excitatory and dark-excitatory zones, whereas complex cells had overlapping zones (Kagan et al. 2003). Eccentricities ranged from 3 to 10°. Receptive fields $>$2° were excluded. We used several methods to estimate receptive field width. For the method based on a cutoff of 1 SD

TABLE 1. *LGN sample statistics*

	Comparison	Mean	Difference	SE	*t*	*P*	*n*
RF width, minarc	Compensated	29	−5.0	0.9	−5.5	<0.001	30
	Uncompensated	34					
RF width, minarc	Compensated	29	−7.0	1.0	−0.7	0.5	30
	Corrected	29					
RF width, minarc	Uncompensated	34	5.7	1.0	5.9	<0.001	30
	Corrected	29					
Amplitude, ips	Compensated	140*	0.1**	0.02	5.4	<0.001	30
	Uncompensated	110*					
Border width, minarc	Compensated	24	−4.9	0.79	−6.1	<0.001	30
	Uncompensated	29					
Slope, ips/minarc	Compensated	22*	0.21**	0.03	7.2	<0.001	30
	Uncompensated	13*					

*Geometric mean. **Arithmetic mean of the log of the ratio, i.e., the mean difference of the log-transformed data; corresponding SEs are for these means. Significance levels are from paired *t*-tests.

of the amplitude values, mean receptive field widths were 39 ± 2 and 43 ± 3 minarc in the compensated and uncompensated V1 data, and 29 ± 2 and 34 ± 2 minarc in compensated and uncompensated LGN data (Tables 1 and 2). Paired comparisons showed that these data sets differed significantly by a shift of 4 or 5 minarc for cortex and LGN ($P < 0.001$, $n = 32$ for cortex and $n = 30$ for LGN, paired *t*-test).

These results were confirmed when fitting Gaussians to the histograms (Read and Cumming 2003). Because some fits were poor, several cells did not yield width values. For the V1 population, means (in minarc) were 45 ± 4 ($n = 24$) and 48 ± 4 ($n = 24$) for compensated and uncompensated conditions, $P = 0.04$, $n = 19$ for the paired comparison. The LGN data gave means of 30 ± 2 ($n = 30$) versus 37 ± 2 ($n = 28$) for the compensated and uncompensated populations, $P < 0.001$, $n = 28$ for the paired *t*-test.

Figure 4, *A* and *B* shows these results, plotting the uncompensated widths against their corresponding compensated widths, distinguishing the two monkeys by color in the cortex plot. Separating the monkeys for the V1 data, the differences between the uncompensated and compensated widths are significant for both monkeys ($P < 0.05$ for M46, $P < 0.001$ for M49). The line of equality is shown here. Regression lines had slopes near 1 (not shown). These results imply that uncompensated eye movements inflate the sizes of receptive fields by a relatively constant amount, independent of their true sizes. This inflation had its most important effects on small fields, which were enlarged by as much as 50%. As receptive fields get larger, the effects of fixational eye movements become relatively less important. However, the average 4 minarc inflation represents a major error for many cells in LGN and V1.

The widths of just the receptive field borders were compared in both conditions. Again, compensation yielded narrower border regions (Tables 1 and 2). Figure 4, *C* and *D* shows that border widths were narrower in the compensated condition. Eye movements smeared the borders of geniculate receptive fields most noticeably. For the cortical data, the edges of the receptive fields often had more gradual slopes and the effects of eye movements were less obvious.

Amplitudes of averaged histograms were measured in compensated and uncompensated conditions. Amplitudes in the compensated runs tended to be higher than those in the uncompensated runs (Fig. 5, *A* and *B*). The geometric mean of the ratio of compensated to uncompensated peak amplitudes for LGN cells was 1.27 ($P < 0.001$, $n = 30$, paired *t*-test; geometric means are appropriate statistics for these ratio data). For the cortical data, the geometric mean ratio of amplitudes was 1.28 ($P < 0.001$, $n = 32$). Amplitudes derived from Gaussian fits yielded similar findings: geometric mean ratio of 1.35 ($P < 0.001$, $n = 28$) for LGN and 1.19 ($P = 0.01$, $n = 19$) for V1. In summary, mean peak response amplitudes in uncompensated conditions were about 80% of what they might be in the absence of eye movements.

The raw slopes of the receptive field profiles, determined by both receptive field width and by response amplitude, were much higher in the compensated than in the uncompensated condition (Fig. 5, *C* and *D*). The difference between compensated and uncompensated conditions is significant (Tables 1

TABLE 2. *VI sample statistics*

	Comparison	Mean	Difference	SE	*t*	*P*	*n*
RF width, minarc	Compensated	39	−3.6	0.78	−4.7	<0.001	32
	Uncompensated	43					
RF width, minarc	Compensated	39	−1.5	1.2	−1.2	0.23	32
	Corrected	41					
RF width, minarc	Uncompensated	43	1.8	1.3	1.4	0.17	32
	Corrected	41					
Amplitude, ips	Compensated	92*	0.1**	0.02	4.7	<0.001	32
	Uncompensated	72*					
Border width, minarc	Compensated	32	−3.3	0.8	−3.9	<0.001	32
	Uncompensated	36					
Slope, ips/minarc	Compensated	10*	0.12**	0.03	4.6	<0.001	32
	Uncompensated	7*					

Conventions are identical to those in Table 1.

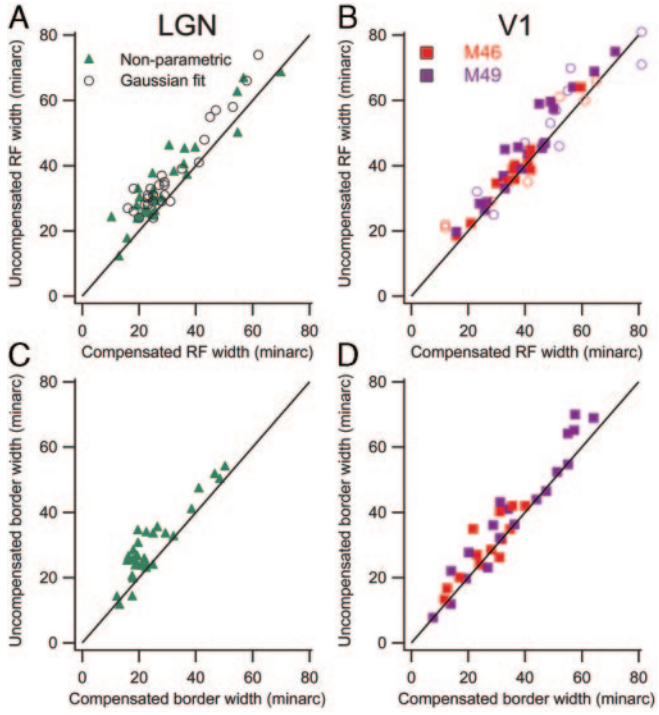

FIG. 4. Population comparisons for receptive field width. *Left*: geniculate data. *Right*: cortical data (distinguishing the 2 monkeys by color). Black lines are lines of equality. *A* and *B*: uncompensated receptive field width is plotted against compensated width. Solid markers show estimates from a relatively nonparametric method and open circles show widths derived from fitting Gaussians to histograms. *C* and *D*: border widths were derived from slopes of normalized histograms.

and 2; $P < 0.001$, $n = 32$ for cortex and $n = 30$ for LGN data, using geometric means). The ratio of compensated to uncompensated slopes was 1.6 in LGN and 1.3 in V1. These slopes determine the maximum sensitivity of neurons to changes of stimulus position, implying that without compensation this sensitivity can be greatly underestimated.

Longer-term stability

Read and Cumming (2003) suggested that the position information from eye coils might degrade slowly as the eye moves over several minutes. We therefore compared the histograms measured at the beginning of each 5- to 20-min run with those measured at the end of the run. We used the first 20 sweeps and the last 20 sweeps and compared the two histograms by computing their correlation. If the average eye position differed between the beginning and end of the run, the histograms would be shifted relative to each other and their correlation would be reduced. An example is shown in Fig. 6, from an LGN cell tested over a period of about 5 min. The solid traces show the histograms compiled from the first 20 sweeps (roughly the initial 2 min) and the dashed traces show the data from the last 20 sweeps. Both directions are shown, for compensated and uncompensated conditions. The correlations between the early and late data were 0.74 and 0.85 for the uncompensated histograms and 0.94 and 0.96 for the compensated histograms. Over the population of LGN cells ($n = 27$ because a few cells were not tested for more than 40 sweeps), the correlation between early and late histograms was significantly smaller for uncompensated than for compensated data ($P < 0.001$, Wilcoxon paired-samples test, medians of 0.79 and 0.89). Only five V1 cells were tested sufficiently for these comparisons. Errors did not accumulate over time in the compensated condition, as further described later with respect to measuring vergence.

Effects of off-line correction for eye position

The uncompensated histograms were corrected for eye position off-line and compared with the uncorrected results. As a result of the correction, spikes that occurred when eye movements translated the receptive field to the position of the bar are shifted back into the receptive field. However, the algorithm cannot replace spikes that were missed because the receptive field was shifted off the stimulus by eye movements. The corrected receptive fields were smaller than the uncorrected receptive fields by 6 minarc for LGN ($P < 0.001$, $n = 30$) and 2 minarc for V1 (not significant, $n = 32$; Tables 1 and 2; Fig. 7) when measured with the method based on a cutoff of 1 SD of the amplitude values. Gaussian fits yielded similar results: $P < 0.001$, $n = 22$ for LGN and a nonsignificant difference for 17 pairs from V1.

The difference between widths calculated using on-line compensation versus off-line correction did not reach statistical significance. Off-line correction thus appears capable of restoring some of the information missing from the raw uncompensated results, although the uncontrolled nature of the stimulus in retinal coordinates causes some information to be irretrievably lost. Amplitudes of corrected histograms tended to be larger than those of the uncompensated histograms but less than those of the compensated histograms, but neither of these effects reached significance except for the uncompensated comparison in LGN cells. The fact that the corrected widths deviate less from the compensated widths than do the uncorrected widths argues that the eye movements do in fact cause smearing of the receptive fields. That is, the corrections take into account the details of the eye movements and demonstrate that changes in eye position cause firing to occur at the wrong time or not to occur at all.

Importance of compensation for resolving receptive field structures

Compensation is important for receptive field size measurements. It is also important for determining the fine structure of receptive fields. This can take many forms, including end-stopping and disparity tuning. Figure 8 illustrates one example from a simple cell tested in both conditions. The cell had a central ON zone flanked by OFF zones. Responses to bright and dark sweeping bars were collected. Figure 8, *A* and *B* shows a single trial with the dark bar, in the compensated condition. The bar swept forward and back across the receptive field six times in each 5-s trial. Despite the excursions of eye position evident in *A*, the responses in *B* occur reliably. Two responses occurred on each sweep, corresponding to the OFF subzones of the receptive field. The averaged histograms are shown in C for both directions and contrasts. Two OFF subzones and a single ON zone between them can be seen for the preferred, upward direction.

This experiment was repeated without compensating for eye position. Figure 8, *D* and *E* illustrates the decreased reliability

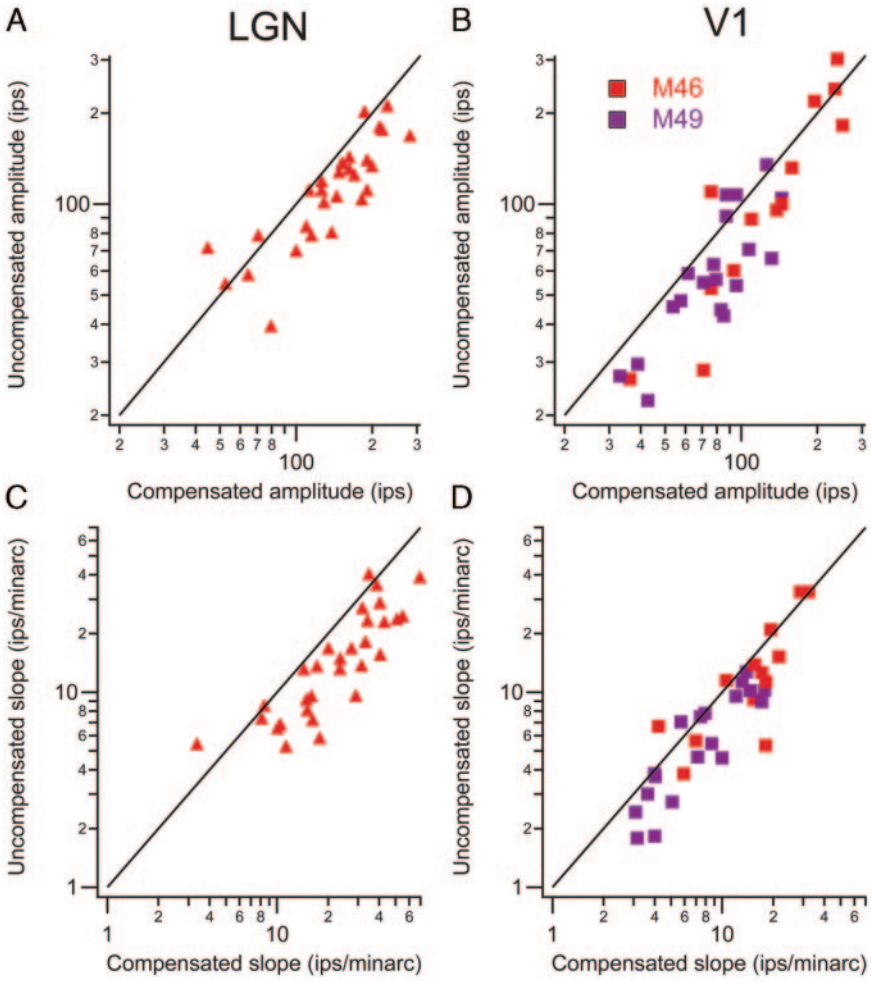

FIG. 5. Population comparisons for amplitude and slope. *A* and *B*: uncompensated vs. compensated amplitudes are plotted. Black line is the equality line. *C* and *D*: uncompensated versus compensated slopes are plotted.

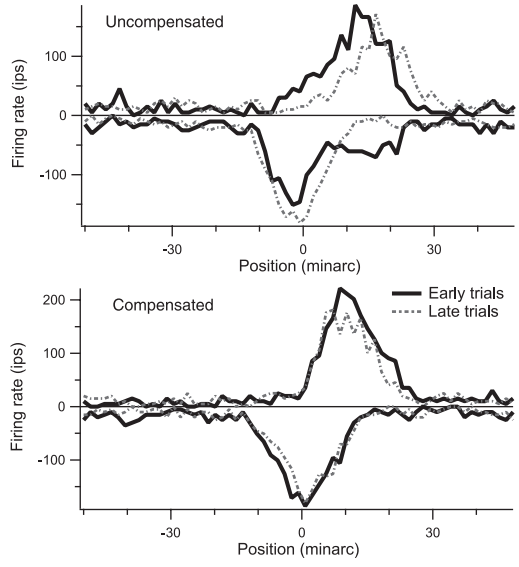

FIG. 6. Example of longer-term measurements of receptive fields. Histograms for responses in both directions (downward direction is inverted) are shown for an LGN P-cell tested in compensated and uncompensated conditions over a time period of 5 min. *Solid traces* arose from the first 20 sweeps in the run and the *dashed traces* from the final 20 sweeps.

evident in one of the trials. The responses of the two OFF zones tend to merge on many sweeps. The averaged histograms show this more clearly. The response to the dark bar is now barely bimodal. Because the response to the bright bar is also smeared, it appears that the cell has broadly overlapping ON and OFF zones, and would be classified as complex.

Beyond the smearing of the subzones, the entire receptive field width is slightly larger in the uncompensated case. The responses to both bright and dark bars were spread over greater extents of space in the uncompensated case (magenta bars and values above the histograms; the differences between the uncompensated and compensated widths were on the order of 6 minarc). Response amplitudes were lower in the uncompensated condition. These changes in amplitude can be caused by a loss of coherence of spikes as well as by failures to evoke spikes. Overall, compensation provides an enhanced view of the receptive field because the stimulus is better controlled.

Measured variability of vergence

As another test of the stability of the eye position measurements, we measured relative horizontal vergence of both monkeys, twice for M46 and six times for M49. In each case, repeated 5-s trials were run over a period of 15–30 min. We computed the SD of the vergence over these runs that encompassed 50–100 trials each. If the eye coil signals were unreliable, these SDs should be large. Vergence behavior is known

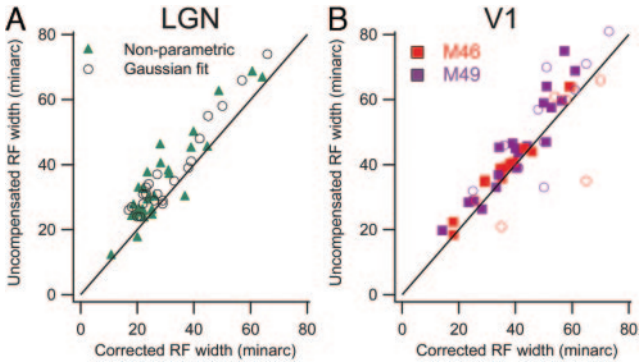

FIG. 7. Effect of off-line correction. Widths from uncompensated runs after correcting for eye position are compared with uncompensated widths. Solid markers show estimates based on the cutoff at 1 SD; open symbols show estimates from Gaussian fits. Black line is the line of equality.

to be highly accurate, so should not mask large eye coil artifacts. Monkeys had a tendency to improve their fixation behavior toward the ends of trials, presumably anticipating the offset of the fixation target that was the cue for their response and subsequent reward. Figure 9*A* illustrates the average behavior over the eight runs. Each point represents the vergence SD for a 500-ms epoch during the trials. Means and SEs are given over the eight runs. By the end of the trial, monkeys were keeping their eyes within 2 minarc of each other across these long runs. Data from one run for M49 are shown in Fig. 9, *B–D*. The vergence ranged over about 4 minarc around the target at a distance of 114 cm (actual convergence of about 2°). Single trials when the monkey looked nearer or farther than the target are illustrated in Fig. 9*C*. Eye movements were largely conjugate. As illustrated in Fig. 9*A*, the trial on the *right* is typical in that the monkey initially did not look directly at the LED, but improved fixation toward the end of the trial in preparation for responding to the offset of the target. For this reason, vergence values in Fig. 9*B* were taken as the mean of the last 0.5 s of each trial, although earlier epochs after the first second are nearly as reliable. Because the eye movements are conjugate, the variance of vergence is smaller than the variance of either eye's position. In other words, fixational instability occurs mostly in the plane normal to the direction of gaze.

For comparison, the SD of vergence for human subjects over a time period of 2 min is about 2 minarc (St. Cyr and Fender 1969). These data suggest that the monkeys are maintaining vergence with an accuracy comparable to that of human subjects. The eye coil signals do not add artifacts that exceed this magnitude, but instead these data are stable over many minutes and are at least as precise as 2 minarc. This is a conservative estimate of the artifact, which appears to be much smaller, perhaps close to the peak-to-peak noise of 0.5 minarc measured in dummy coils. It is difficult to give more precise estimates of errors in the eye position measurements because these values are smaller than the resolution used in stimulus generation and receptive field sizes for the current data.

DISCUSSION

Monkeys, like people, make small eye movements during fixation even when highly trained in fixation tasks. Because receptive fields in primary visual cortex are fixed in retinal coordinates, eye movements in alert monkeys can blur the measured receptive field and result in underestimates of the spatial resolution of neurons. Eye position varied over about 20 minarc during fixation. These seemingly minor deviations can have important effects on receptive field measurements, creating on average about 4 minarc increases in width and 20% decreases in amplitude. Our results probably underestimate the full effects of eye movements on the neuronal responses

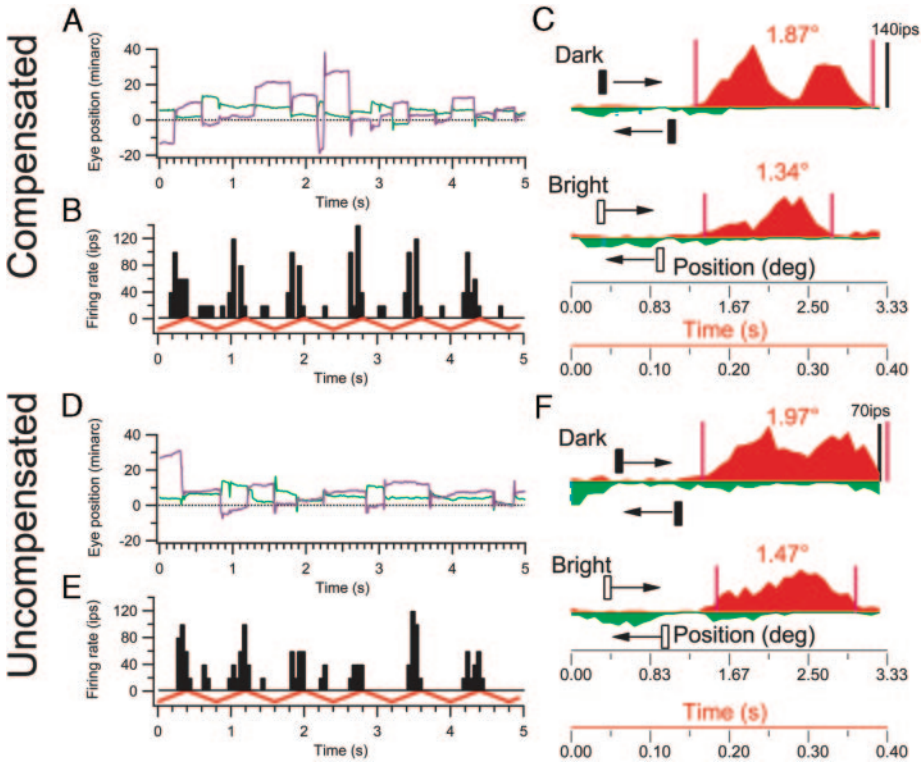

FIG. 8. Advantages of compensation for eye position in receptive field mapping. A layer 3 simple cell was tested with bright and dark bars drifting up and down in compensated (*A*, *B*, *C*) and uncompensated (*D*, *E*, *F*) conditions. Horizontal (green) and vertical (magenta) eye positions are shown for single trials in *A* and *D*. Stimulus (red in *B* and *E*) drifted upward and downward across the receptive field at 8.33°/s. Histograms for both directions, contrasts, and compensation conditions averaged over 9 trials are shown in *C* and *F*. Nonpreferred direction responses are plotted downward and inverted in time. Horizontal axis scales are shown both in time and space and calibration bars are shown for the firing rates. Magenta bars show the limits of the receptive fields and the widths are given for the preferred direction.

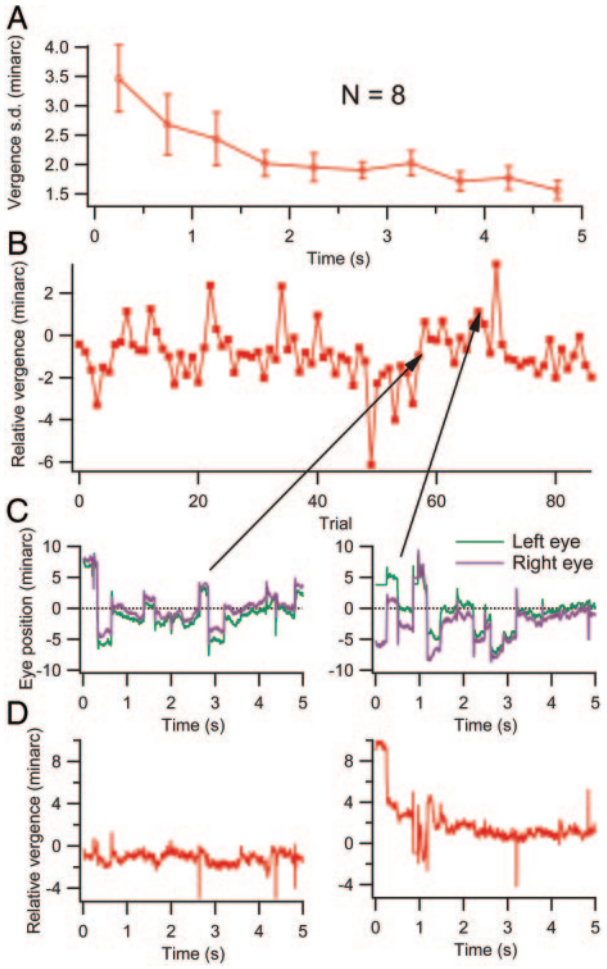

FIG. 9. Vergence measurements. *A*: SD of relative vergence over 15- to 30-min runs is shown for each 500-ms epoch during the trials. Data points and error bars are means and SEs over 8 runs, with 50–100 trials in each run, a total of 650 trials. Monkeys tended to fixate best at the end of the trial, to respond when the fixation target disappeared. *B*: relative vergence is plotted for a series of 5-s trials in a 30-min run. Values are means over the final 500 ms of each trial. *C*: 2 trials illustrate the monocular eye positions. On the *left*, the monkey fixated slightly behind the fixation target and on the *right* slightly in front of the target. *D*: vergence is plotted for each of the trials in *C*.

because we did not eliminate saccades, which were only partially compensated because of their speed. Furthermore, many animals may not fixate as well as the two monkeys we tested, particularly M46.

Read and Cumming (2003) suggested that correcting for eye movements using the scleral search coil did not in general produce smaller receptive field estimates and that there are artifacts in eye position measurement with this procedure. To evaluate the effectiveness and accuracy of this eye coil system in detail, we sutured the eye coils to the sclera and applied stimulus compensation. We compared results with and without compensation and found that compensated receptive field widths were smaller, whereas amplitude and slope were higher than in the uncompensated case. Noise from dummy coils was negligible compared with eye movement signals. Eye position measurements were stable over 0.5-h runs. The SD of vergence was 1–3 minarc, similar to humans, and less than half the value found by Read and Cumming, 12 and 5.3 minarc for two pairs of eye coils. The fact that Read and Cumming did not find a positive influence of compensation may be the result of not suturing the eye coils to the globe. This allows slippage of the coil during large eye movements and the coil does not come to rest at the same location after each movement. Suturing the eye coils to the sclera avoids this artifact and thus provides more accurate estimates of eye position. Additional care must be taken not only to avoid artifacts from movements of the coil leads, but also to minimize noise from the electronics. We could not obtain an estimate of the size of the artifacts from the monkey eye coils because they appear to be smaller than any size measurement we made. The finest scale tested here was the approximately 2 minarc deviations of vergence. We expect that these artifacts are only slightly larger than the noise observed in dummy coils, on the order of 0.5 minarc. The main source of noise not seen with dummy coils is from muscle movements. We tried computing the size of the artifact by several methods, but the resolution of our measurements was insufficient to yield reliable estimates.

Some investigators corrected stimulus position off-line instead of on-line (Conway 2001; Livingstone 1998; Livingstone and Tsao 1999; Livingstone et al. 1996; Tsao et al. 2003). They observed improved resolution in some cells but not in others after performing off-line corrections. We found that off-line correction substantially improves receptive field estimates, as suggested by Livingstone and Tsao (1999). Off-line correction uses the eye position records to build histograms showing where the stimulus was positioned when spikes were evoked. The actual stimulus, however, was not compensated, so that its position on the retina during the experiment still jumped with eye movements. In addition, eye velocity is not taken into account and spikes that the uncontrolled stimulus failed to evoke cannot be recovered. Care must be taken to build into the correction algorithm appropriate compensations for the jittery nature of stimulus movement on the retina.

In addition to measurements of receptive field dimensions, compensation is critical for accurate assays of numerous V1 properties, especially for cells with small receptive fields. Even small eye jitter can cause large changes in responses and reliability of neuronal processing can be underestimated if eye movements are not factored into the measurements (Gur et al. 1997). These problems are particularly acute in the foveal representation, where receptive fields are tiny, and little knowledge of their physiology is available. Compensating for eye movements can reduce the bias toward large receptive field cells present in most studies.

Cells in layer 3 of V1, even outside the foveal representation, usually have small receptive fields and often are both direction selective and end-stopped. Without eye position compensation, these cells are especially difficult to characterize, and some direction selective cells appear to be less selective because eye movements occasionally provide preferred retinal image motion even when the stimulus moves in the nonpreferred direction in space.

On the other hand, these results point to the issue of how we see in the presence of eye movements. In natural situations, individual neurons will not receive identical stimulation from moment to moment because of effects of eye and body movements (self-motion). Presumably, the correlations among cells that are generated by self-motion, which provides common

motion across the visual field, are used to recover the information that is experimentally observable in single cells using position compensation.

REFERENCES

Barash S, Melikyan A, Sivakov A, Tauber M. Shift of visual fixation dependent on background illumination. *J Neurophysiol* 79: 2766–2781, 1998.

Gur M, Beylin A, **Snodderly DM.** Response variability of neurons in primary visual cortex (V1) of alert monkeys. *J Neurosci* 17: 2914–2920, 1997.

Gur M, Snodderly DM. Studying striate cortex neurons in behaving monkeys: benefits of image stabilization. *Vision Res* 27: 2081–2087, 1987.

Gur M, Snodderly DM. Visual receptive fields of neurons in primary visual cortex (V1) move in space with the eye movements of fixation. *Vision Res* 37: 257–265, 1997.

Judge SJ, Richmond BJ, **Chu FC.** Implantation of magnetic search coils for measurement of eye position: an improved method. *Vision Res* 20: 535–538, 1980.

Kagan I, Gur M, Snodderly DM. Spatial organization of receptive fields of V1 neurons of alert monkeys: comparison with responses to gratings. *J Neurophysiol* 88: 2557–2574, 2002.

Livingstone M, Freeman D, Hubel D. Visual responses in V1 of freely viewing monkeys. *Cold Spring Harb Symp Quant Biol* 61: 27–37, 1996.

Livingstone MS. Mechanisms of direction selectivity in macaque V1. *Neuron* 20: 509–526, 1998.

Livingstone MS, Tsao DY. Receptive fields of disparity-selective neurons in macaque striate cortex. *Nat Neurosci* 2: 825–832, 1999.

Read JC, Cumming BG. Measuring V1 receptive fields despite eye movements in awake monkeys. *J Neurophysiol* 90: 946–960, 2003.

Reitboeck HJ. Fiber microelectrodes for electrophysiological recordings. *J Neurosci Methods* 8: 249–262, 1983.

Robinson DA. A method of measuring eye movement using scleral search coil in a magnetic field. *IEEE Trans Biomed Eng* 10: 137–145, 1963.

Snodderly DM. Effects of light and dark environments on macaque and human fixational eye movements. *Vision Res* 27: 401–415, 1987.

St. Cyr GJ, Fender DH. The interplay of drifts and flicks in binocular fixation. *Vision Res* 9: 245–265, 1969.

Tsao DY, Conway BR, Livingstone MS. Receptive fields of disparity-tuned simple cell in macaque V1. *Neuron* 38: 103–114, 2003.